- Polymersome Colloidosomes for Enzyme Catalysis in a Biphasic System
  Wang, Z.; van Oers, M. C. M.; Rutjes, F. P. J. T.; van Hest, J. C. M. *Angew. Chem. Int. Ed.* **2012**, *51*, 10746–10750.
  Abstract:

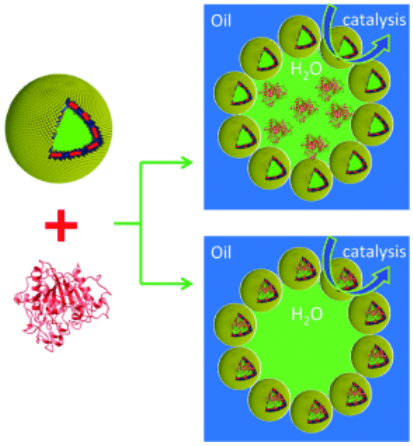

A polymersome-stabilized Pickering emulsion was prepared and applied in a biphasic enzymatic reaction. This type of Pickering emulsion was stabilized by fully packed crosslinked polymersomes at the water/oil interface. CalB, as a model enzyme (red ribbon structure), was loaded either in the water phase or in the lumen of the polymersomes of the Pickering emulsion (see picture), which highly enhanced its catalytic performance and recyclability.

- Transition Metal Complexes of Anionic N-Heterocyclic Dicarbene Ligands
  Musgrave, R. A.; Turbervill, R. S. P.; Irwin, M.; Goicoechea, J. M. *Angew. Chem. Int. Ed.* **2012**, *51*, 10832–10835.
  Abstract:

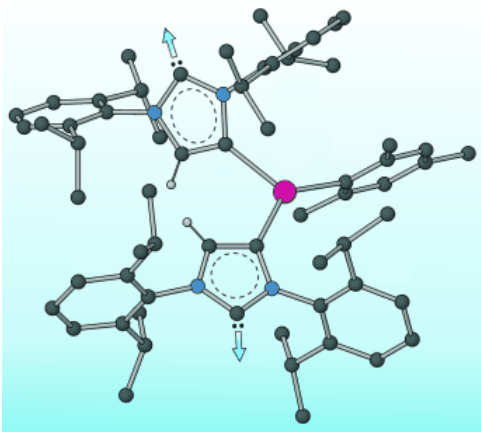

A tale of two carbenes: Reaction of :C[N(2,6-*i*$Pr_2C_6H_3$)CH]$_2$ (IPr) with $Mn_3(mes)_6$ (mes=2,4,6-trimethylphenyl) yielded the trigonal planar complex [Mn(IPr)$(mes)_2$]. Reduction of this species with potassium/graphite in THF afforded the polymeric dicarbene-bridged species K[{:C[N(2,6-*i*$Pr_2C_6H_3$)]$_2$(CH)C}$_2$Mn(mes)(thf)]·THF (see picture). The anionic moiety in this complex is the first reported example of a transition metal complex containing an N-heterocyclic dicarbene ligand. Gray C, blue N, red Mn.

- Thermally Assisted Photonic Inversion of Supramolecular Handedness

Gopal, A.; Hifsudheen, M.; Furumi, S.; Takeuchi, M.; Ajayaghosh, A. *Angew. Chem. Int. Ed.* **2012**, *51*, 10505–10509.

Abstract:

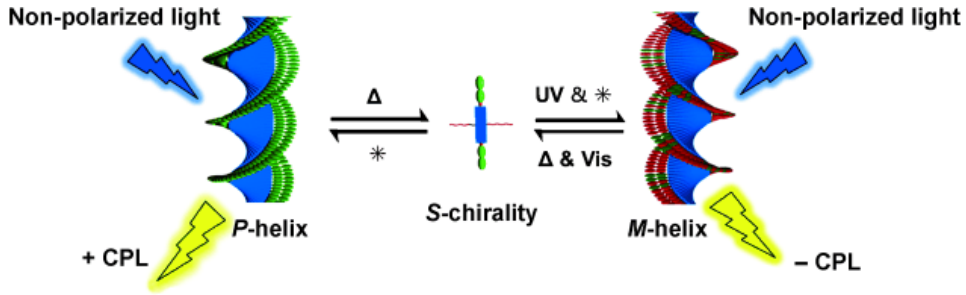

Spiraling into control: A photoresponsive supramolecular assembly demonstrates that light, along with heating (Δ) and cooling (), can cause chiral communication between molecules. This effect leads to bias in the helicity of the complex, causing a reversible switching of macroscopic handedness, as shown by a reversal of sign of the circularly polarized luminescence (CPL) that is emitted.

- Kinetic Resolution of Nitrogen Heterocycles with a Reusable Polymer-Supported Reagent
  Kreituss, I.; Murakami, Y.; Binanzer, M.; Bode, J. W. An*gew. Chem. Int. Ed.* **2012**, *51*, 10660–10663.
  Abstract:

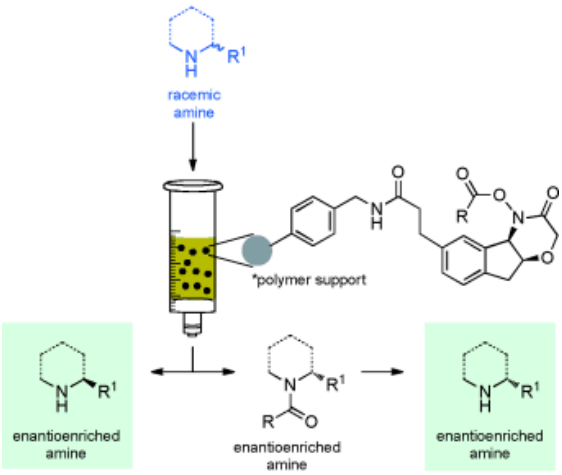

Shake it up baby! Simply shaking a polymer-supported reagent and the racemic amine at room temperature kinetically resolves a broad range of N-heterocycles with good selectivity. The polymer-supported reagents are robust, easy to regenerate, and can be reused dozens of times. Cleavable acyl groups can be used to give access to both amine enantiomers in a single resolution.

- Complexation between triptycene-based macrotricyclic host and π-extended viologens: formation of supramolecular poly[3]pseudorotaxanes
  Han, Y.; Gu, Y.-K.; Xiang, J.-F; Chen, C.-F. *Chem. Commun.* **2012**, *48,* 11076–11078.
  Abstract:

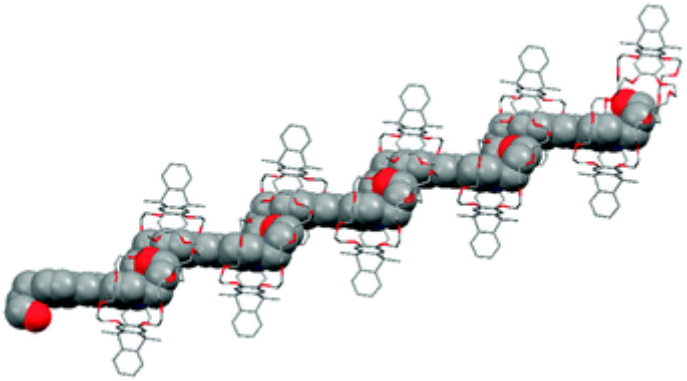

Triptycene-based macrotricyclic host containing two dibenzo-30-crown-10 moieties could form ladder-like supramolecular poly[3]pseudorotaxanes with π-extended viologens in both high concentration solution and solid state.

- Strain-induced delamination of edge-grafted graphite
  Choi, E.-K.; Jeon, I.-Y.; Shin, Y.-R.; Baek, J.-B. *Chem. Commun.* **2012**, *48,* 11109–11111.
  Abstract:

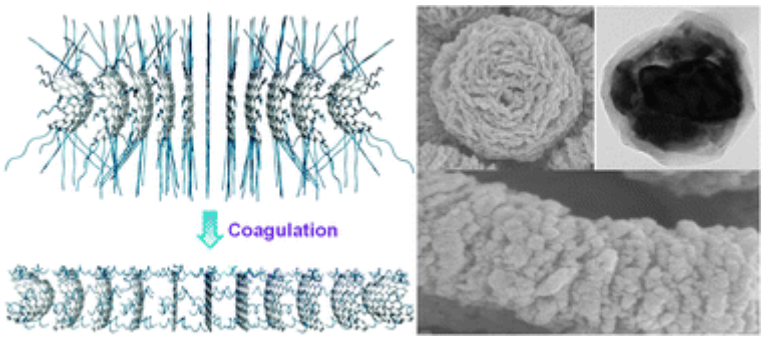

Edge-selectively grafted graphite (EGG) with poly(ether-ketone) was prepared by the Friedel–Crafts acylation in a mild polyphosphoric acid (PPA)–phosphorous pentoxide (P_2O_5) mixture. The homogeneous reaction dope was coagulated in air moisture at different temperatures. The morphology of expanded EGG was changed from balls, balls/rods and rods with respect to coagulation temperatures of 80, 60, 40 and 25 °C, respectively.

- Supramolecular Assembly of Diplatinum Species through Weak PtII···PtII Intermolecular Interactions: A Combined Experimental and ComputationalStudy
  Pérez Paz, A.; Espinosa Leal, L. A.; Azani, M.-R.; Guijarro, A.; Sanz Miguel, P. J.; Givaja, G.; Castillo, O.; Mas-Ballesté, R.; Zamora, F.; Rubio, A. *Chem. Eur. J.* **2012**, *18*, 13787 – 13799.
  Abstract:

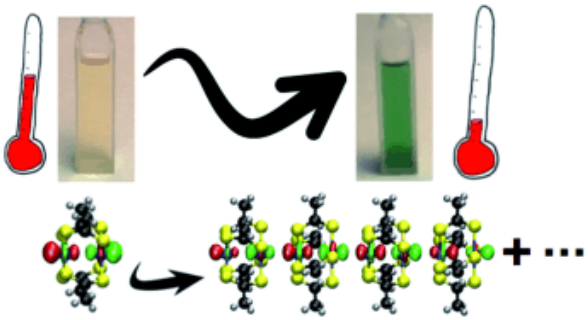

The present study elucidates the factors that govern the spontaneous self-assembly of a family of dimetal $[Pt_2L_4]$ (L=dithiocarboxylato ligand) complexes. Experimental data show that variables such as

temperature, concentration, solvent and the nature of the ligand L have a critical effect on the reversible self-assembly of supramolecular $[Pt_2L_4]n$ entities. In solution, new UV/Vis spectroscopic features emerge at low temperatures and/or high concentrations, which are attributed to the formation of oligomeric $[Pt_2L_4]n$ species. The description of intermolecular Pt···Pt interactions, the main driving force for the association, was addressed from a computational perspective. The contributions from intermolecular Pt···S and S···S interactions to these supramolecular assemblies were found to be repulsive. Experimental UV/Vis data have been interpreted by means of computational spectroscopy.

- Ultrafast Photoinduced Energy and Electron Transfer in Multi-Modular Donor–Acceptor Conjugates
  El-Khouly, M. E.; Wijesinghe, C.A.; Nesterov, V. N.; Zandler, M. E.; Fukuzumi, S.; D'Souza, F. *Chem. Eur. J.* **2012**, *18*, 13844 – 13853.
  Abstract:

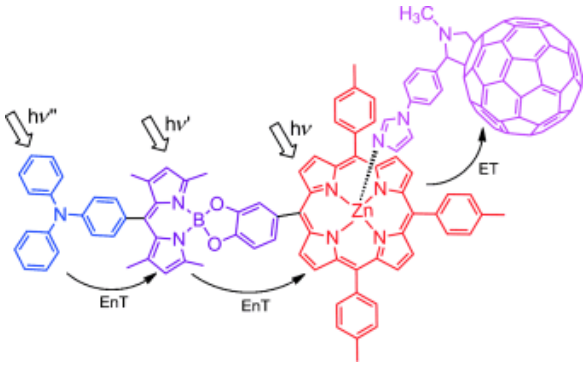

New multi-modular donor–acceptor conjugates featuring zinc porphyrin (ZnP), catechol-chelated boron dipyrrin (BDP), triphenylamine (TPA) and fullerene (C_{60}), or naphthalenediimide (NDI) have been newly designed and synthesized as photosynthetic antenna and reaction-center mimics. The X-ray structure of triphenylamine-BDP is also reported. The wide-band capturing polyad revealed ultrafast energy-transfer (k_{ENT}=1.0×10^{12} s^{-1}) from the singlet excited BDP to the covalently linked ZnP owing to close proximity and favorable orientation of the entities. Introducing either fullerene or naphthalenediimide electron acceptors to the TPA-BDP-ZnP triad through metal–ligand axial coordination resulted in electron donor–acceptor polyads whose structures were revealed by spectroscopic, electrochemical and computational studies. Excitation of the electron donor, zinc porphyrin resulted in rapid electron-transfer to coordinated fullerene or naphthalenediimide yielding charge separated ion-pair species. The measured electron transfer rate constants from femtosecond transient spectral technique in non-polar toluene were in the range of 5.0×10^{9}–3.5×10^{10} s^{-1}. Stabilization of the charge-separated state in these multi-modular donor–acceptor polyads is also observed to certain level.

- Azobenzene Polyesters Used as Gate-Like Scaffolds in Nanoscopic Hybrid Systems
  Bernardos, A.; Mondragón, L.; Javakhishvili, I.; Mas, N.; de la Torre, C.; Martínez-Máñez, R.; Sancenón, F.; Barat, J. M.; Hvilsted, S.; Orzaez, M.; Pérez-Payá, E.; Amorós, P. *Chem. Eur. J.* **2012**, *18*, 13068–13078.
  Abstract:

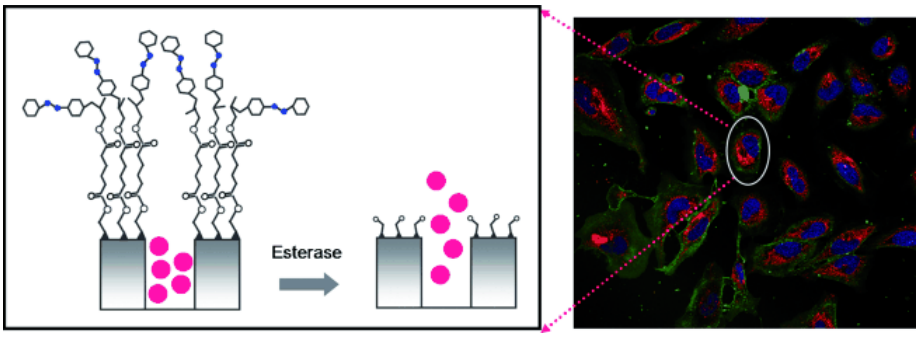

The synthesis and characterisation of new capped silica mesoporous nanoparticles for on-command delivery applications is reported. Functional capped hybrid systems consist of MCM-41 nanoparticles functionalised on the external surface with polyesters bearing azobenzene derivatives and rhodamine B inside the mesopores. Two solid materials, Rh-PAzo8-S and Rh-PAzo6-S, containing two closely related polymers, PAzo8 and PAzo6, in the pore outlets have been prepared. Materials Rh-PAzo8-S and Rh-PAzo6-S showed an almost zero release in water due to steric hindrance imposed by the presence of anchored bulky polyesters, whereas a large delivery of the cargo was observed in the presence of an esterase enzyme due to the progressive hydrolysis of polyester chains. Moreover, nanoparticles Rh-PAzo8-S and Rh-PAzo6-S were used to study the controlled release of the dye in intracellular media. Nanoparticles were not toxic for HeLa cells and endocytosis-mediated cell internalisation was confirmed by confocal microscopy. Furthermore, the possible use of capped materials as a drug-delivery system was demonstrated by the preparation of a new mesoporous silica nanoparticle functionalised with PAzo6 and loaded with the cytotoxic drug camptothecin (CPT-PAzo6-S). Following cell internalisation and lysosome resident enzyme-dependent gate opening, CPT-PAzo6-S induced CPT-dependent cell death in HeLa cells.

- Synthesis of Deoxynucleoside Triphosphates that Include Proline, Urea, or Sulfonamide Groups and Their Polymerase Incorporation into DNA
  Hollenstein, M. *Chem. Eur. J.* **2012**, *18*, 13320–13330.
  Abstract:

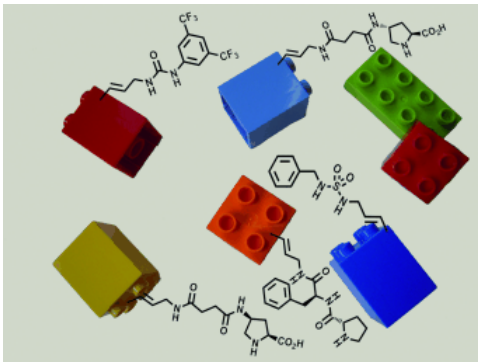

To expand the chemical array available for DNA sequences in the context of in vitro selection, I present herein the synthesis of five nucleoside triphosphate analogues containing side chains capable of organocatalysis. The synthesis involved the coupling of L-proline-containing residues (dU^{tP}TP and dU^{cP}TP), a dipeptide (dU^{FP}TP), a urea derivative (dU^{Bpu}TP), and a sulfamide residue (dU^{Bs}TP) to a suitably protected common intermediate, followed by triphosphorylation. These modified dNTPs were shown to be excellent substrates for the Vent (*exo*$^-$) and *Pwo* DNA polymerases, as well as the Klenow fragment of *E. coli* DNA polymerase I, although they were only acceptable substrates for the 9°N_m polymerase. All of the modified dNTPs, with the exception of

$dU^{Bpu}TP$, were readily incorporated into DNA by the polymerase chain reaction (PCR). Modified oligonucleotides efficiently served as templates for PCR for the regeneration of unmodified DNA. Thermal denaturation experiments showed that these modifications are tolerated in the major groove. Overall, these heavily modified dNTPs are excellent candidates for SELEX.

- Self-Assembled Colloidal Superparticles from Nanorods
  Wang, T.; Zhuang, J.; Lynch, J.; Chen, O.; Wang, Z.; Wang, X.; LaMontagne, D.; Wu, H.; Wang, Z.; Cao, Y. C. *Science* **2012**, *338*, 358-363.
  Abstract:

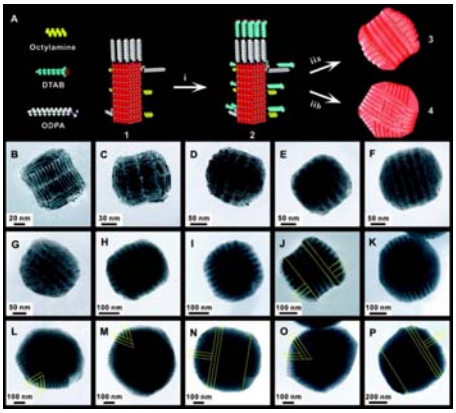

Colloidal superparticles are nanoparticle assemblies in the form of colloidal particles. The assembly of nanoscopic objects into mesoscopic or macroscopic complex architectures allows bottom-up fabrication of functional materials. We report that the self-assembly of cadmium selenide-cadmium sulfide (CdSe-CdS) core-shell semiconductor nanorods, mediated by shape and structural anisotropy, produces mesoscopic colloidal superparticles having multiple well-defined supercrystalline domains. Moreover, functionality-based anisotropic interactions between these CdSe-CdS nanorods can be kinetically introduced during the self-assembly and, in turn, yield single-domain, needle-like superparticles with parallel alignment of constituent nanorods. Unidirectional patterning of these mesoscopic needle-like super particles gives rise to the lateral alignment of CdSe-CdS nanorods into macroscopic, uniform, freestanding polymer films that exhibit strong photoluminescence with a striking anisotropy, enabling their use as downconversion phosphors to create polarized light-emitting diodes.

- Initiation of transcription-coupled repair characterized at single-molecule resolution
  Howan, K.; Smith, A. J.; Westblade, L. F.; Joly, N.; Grange, W.; Zorman, S.; Darst, S. A.; Savery, N. J.; Strick, T. R. *Nature* **2012**, *490*, 431-434.
  Abstract:

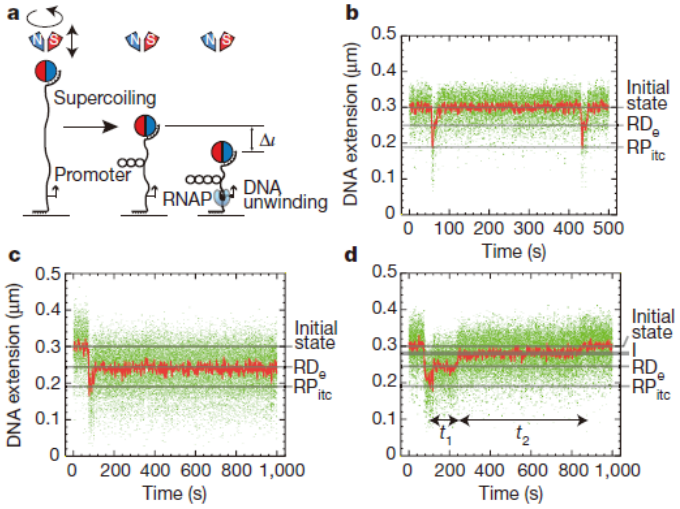

Transcription-coupled DNA repair uses components of the transcription machinery to identify DNA lesions and initiate their repair. These repair pathways are complex, so their mechanistic features remain poorly understood. Bacterial transcription coupled repair is initiated when RNA polymerase stalled at a DNA lesion is removed by Mfd, an ATP-dependent DNA translocase. Here we use single-molecule DNA nanomanipulation to observe the dynamic interactions of *Escherichia coli* Mfd with RNA polymerase elongation complexes stalled by a cyclopyrimidine dimer or by nucleotide starvation. We show that Mfd acts by catalysing two irreversible, ATP-dependent transitions with different structural, kinetic and mechanistic features. Mfd remains bound to the DNA in a long-lived complex that could act as a marker for sites of DNA damage, directing assembly of subsequent DNA repair factors. These results provide a framework for considering the kinetics of transcription-coupled repair *in vivo*, and open the way to reconstruction of complete DNA repair pathways at single molecule resolution.

- Facile Fabrication and High Photoelectric Properties of Hierarchically Ordered Porous TiO_2
  Sun, W.; Zhou, S.; You, B.; Wu, L. *Chem. Mater.* **2012**, *24*, 3800–3810.
  <u>Abstract:</u>

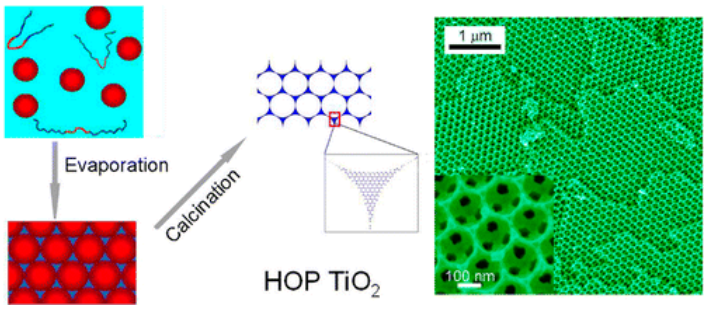

This paper presents the first successful fabrication of hierarchically ordered porous (HOP) TiO_2. Poly(styrene-*co*-acrylic acid) colloidal spheres and triblock copolymer P123 were used as macro- and mesoporous structure-directing agents, and titanium chloride and titanium tetraisopropoxide were used as sources of titania. When the mixture of polymer spheres, P123, and titania precursors were cast on substrates, and conducted for complete solvent evaporation, followed by thermal treatment, large-scale HOP TiO_2 can be directly fabricated. The *in situ* chelate effect between the titania precursors and the poly(styrene-*co*-acrylic acid) plays a key role in the fabrication of HOP TiO_2. The as-obtained HOP TiO_2 exhibits 50% and 70% greater the highest photocurrent under UV and visible lights, respectively, and far higher photoelectrocatalytic property than commercial TiO_2 (P-25).

- Thermosensitive Multilayer Hydrogels of Poly(*N*-vinylcaprolactam) as Nanothin Films and Shaped Capsules
  Liang, X.; Kozlovskaya, V.; Chen, Y.; Zavgorodnya, O.; Kharlampieva, E. *Chem. Mater.* **2012**, *24*, 3707–3719.
  Abstract:

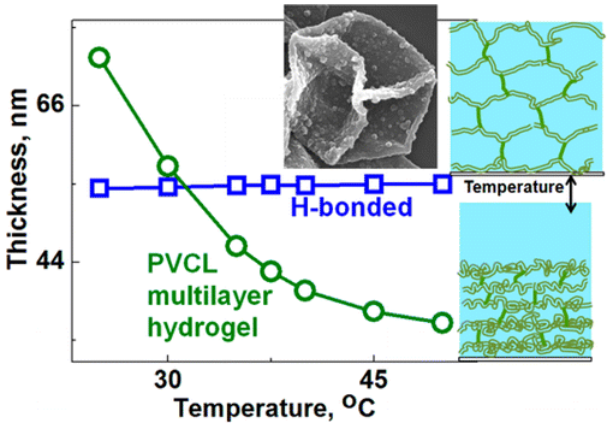

We report on nanothin multilayer hydrogels of cross-linked poly(*N*-vinylcaprolactam) (PVCL) that exhibit distinctive and reversible thermoresponsive behavior. The single-component PVCL hydrogels were produced by selective cross-linking of PVCL in layer-by-layer films of PVCL-NH_2 copolymers assembled with poly(methacrylic acid) (PMAA) via hydrogen bonding. The degree of the PVCL hydrogel film shrinkage, defined as the ratio of wet thicknesses at 25 to 50 °C, was demonstrated to be 1.9 ± 0.1 and 1.3 ± 0.1 for the films made from PVCL-NH_2-7 and PVCL-NH_2-14 copolymers, respectively. No temperature-responsive behavior was observed for noncross-linked two-component films because of the presence of PMAA. We also demonstrated that temperature-sensitive PVCL capsules of cubical and spherical shapes could be fabricated as hollow hydrogel replicas of inorganic templates. The cubical $(PVCL)_7$ capsules retained their cubical shape when temperature was elevated from 25 to 50 °C exhibiting 21 ± 1% decrease in the capsule size. Spherical hydrogel capsules demonstrated similar shrinkage of 23 ± 1%. The temperature-triggered capsule size changes were completely reversible. Our work opens new prospects for developing biocompatible and nanothin hydrogel-based coatings and containers for temperate-regulating drug delivery, cellular uptake, sensing, and transport behavior in microfluidic devices.

- Uncovering Molecular Details of Urea Crystal Growth in the Presence of Additives
  Salvalaglio, M.; Vetter, T.; Giberti F.; Mazzotti, M.; Parrinello, M. *J. Am. Chem. Soc.* **2012**, *134*, 17221–17233.
  Abstract:

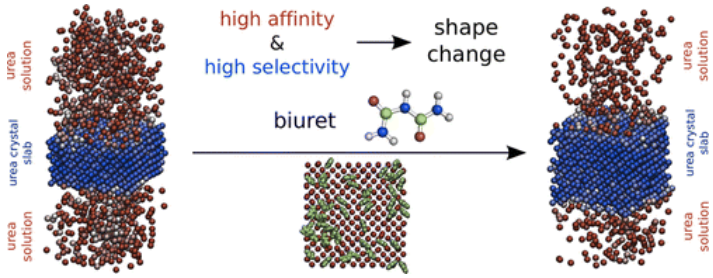

Controlling the shape of crystals is of great practical relevance in fields like pharmacology and fine chemistry. Here we examine the paradigmatic case of urea which is known to crystallize from water

with a needle-like morphology. To prevent this undesired effect, inhibitors that selectively favor or discourage the growth of specific crystal faces can be used. In urea the most relevant faces are the {001} and the {110} which are known to grow fast and slow, respectively. The relevant growth speed difference between these two crystal faces is responsible for the needle-like structure of crystals grown in water solution. To prevent this effect, additives are used to slow down the growth of one face relative to another, thus controlling the shape of the crystal. We study the growth of fast {001} and slow {110} faces in water solution and the effect of shape controlling inhibitors like biuret. Extensive sampling through molecular dynamics simulations provides a microscopic picture of the growth mechanism and of the role of the additives. We find a continuous growth mechanism on the {001} face, while the slow growing {110} face evolves through a birth and spread process, in which the rate-determining step is the formation on the surface of a two-dimensional crystalline nucleus. On the {001} face, growth inhibitors like biuret compete with urea for the adsorption on surface lattice sites; on the {110} face instead additives cannot interact specifically with surface sites and play a marginal sterical hindrance of the crystal growth. The free energies of adsorption of additives and urea are evaluated with advanced simulation methods (well-tempered metadynamics) allowing a microscopic understanding of the selective effect of additives. Based on this case study, general principles for the understanding of the anisotropic growth of molecular crystals from solutions are laid out. Our work is a step toward a rational development of novel shape-affecting additives.

- Gold Nanoparticles as Electronic Bridges for Laccase-Based Biocathodes
  Gutiérrez-Sánchez, C.; Pita, M.; Vaz-Domínguez, C.; Shleev, S.; De Lacey, A. L. *J. Am. Chem. Soc.* **2012**, *134*, 17212–17220.
  Abstract:

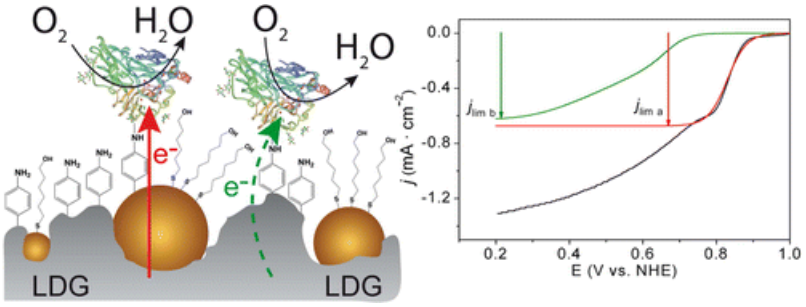

Direct electron transfer (DET) reactions between redox enzymes and electrodes can be maximized by oriented immobilization of the enzyme molecules onto an electroactive surface modified with functionalized gold nanoparticles (AuNPs). Here, we present such strategy for obtaining a DET-based laccase (Lc) cathode for O_2 electroreduction at low overpotentials. The stable nanostructured enzymatic electrode is based on the step-by-step covalent attachment of AuNPs and Lc molecules to porous graphite electrodes using the diazonium salt reduction strategy. Oriented immobilization of the enzyme molecules on adequately functionalized AuNPs allows establishing very fast DET with the electrode via their Cu T1 site. The measured electrocatalytic waves of O_2 reduction can be deconvoluted into two contributions. The one at lower overpotentials corresponds to immobilized Lc molecules that are efficiently wired by the AuNPs with a heterogeneous electron transfer rate constant k_0 ⋙400 s^{-1}.

- Self-Assembly of a [2]Pseudorota[3]catenane in Water
  Forgan, R. S.; Gassensmith, J. J.; Cordes, D. B.; Boyle, M. M.; Hartlieb, K. J.; Friedman, D. C.; Slawin, A. M. Z.; Stoddart, J. F. *J. Am. Chem. Soc.* **2012**, *134*, 17007–17010.

Abstract:

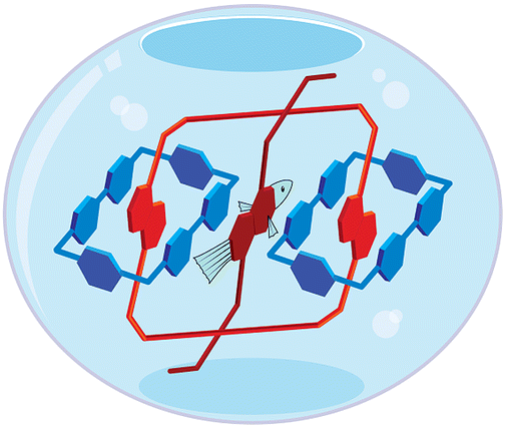

A donor–acceptor [3]catenane incorporating two cyclobis(paraquat-p-phenylene) rings linked together by a dinaphtho[50]crown-14 macrocycle possesses a π-electron-deficient pocket. Contrary to expectation, negligible binding of a hexaethylene glycol chain interrupted in its midriff by a π-electron-rich 1,5-dioxynaphthalene unit was observed in acetonitrile. However, a fortuitous solid-state superstructure of the expected 1:1 complex revealed its inability to embrace any stabilizing [C–H···O] interactions between the clearly unwelcome guest and the host reluctantly accommodating it. By contrast, in aqueous solution, the 1:1 complex becomes very stable thanks to the intervention of hydrophobic bonding.

- Synthesis of a Modified PC70BM and Its Application as an Electron Acceptor with Poly(3-hexylthiophene) as an Electron Donor for Efficient Bulk Heterojunction Solar Cells
  Singh, S. P.; Kumar, Ch. P.; Sharma, G. D.; Kurchania, R.; Roy, M. S. *Adv. Funct. Mater.* **2012**, *22*, 4087–4095.
  Abstract:

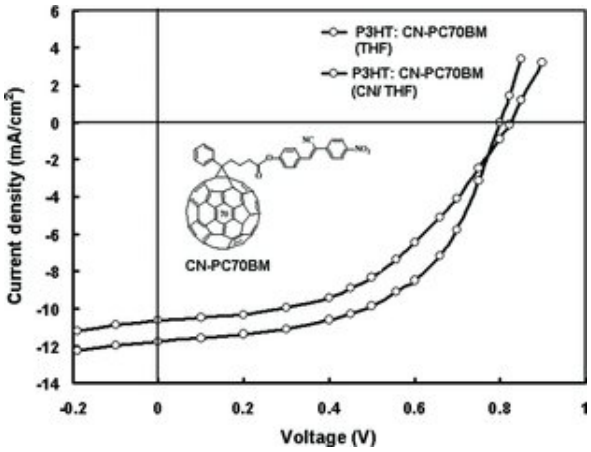

A simple and effective modification of phenyl-C_{70}-butyric acid methyl ester ($PC_{70}BM$) is carried out in a single step after which the material is used as electron acceptor for bulk heterojunction polymer solar cells (PSCs). The modified $PC_{70}BM$, namely CN-$PC_{70}BM$, showed broader and stronger absorption in the visible region (350–550 nm) of the solar spectrum than $PC_{70}BM$ because of the presence of a cyanovinylene 4-nitrophenyl segment. The lowest unoccupied molecular energy level (LUMO) of CN-$PC_{70}BM$ is higher than that of $PC_{70}BM$ by 0.15 eV. The PSC based on the blend (cast from tetrahydrofuran (THF) solution) consists of P3HT as the electron donor and CN-$PC_{70}BM$ as the electron acceptor and shows a power conversion efficiency (PCE) of 4.88%, which is higher than that of devices based on $PC_{70}BM$ as the electron acceptor (3.23%). The higher PCE of the solar cell based

on P3HT:CN-$PC_{70}BM$ is related to the increase in both the short circuit current (J_{sc}) and the open circuit voltage (V_{oc}). The increase in J_{sc} is related to the stronger light absorption of CN-$PC_{70}BM$ in the visible region of the solar spectrum as compared to that of $PC_{70}BM$. In other words, more excitons are generated in the bulk heterojunction (BHJ) active layer. On the other hand, the higher difference between the LUMO of CN-$PC_{70}BM$ and the HOMO of P3HT causes an enhancement in the V_{oc}. The addition of 2% (v/v) 1-chloronapthalene (CN) to the THF solvent during film deposition results in an overall improvement of the PCE up to 5.83%. This improvement in PCE can be attributed to the enhanced crystallinity of the blend (particularly of P3HT) and more balanced charge transport in the device.

- Synthesis and Structure–Property Correlations of Dicyanovinyl-Substituted Oligoselenophenes and their Application in Organic Solar Cells
  Haid, S.; Mishra, A.; Weil, M.; Uhrich, C.; Pfeiffer, M.; Bäuerle, P. *Adv. Funct. Mater.* **2012**, *22*, 4322–4333.
  Abstract:

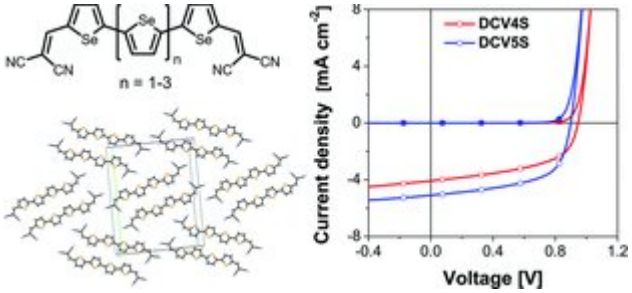

The convergent synthesis of a series of acceptor–donor–acceptor (A-D-A) type dicaynovinyl (DCV)-substituted oligoselenophenes DCV*n*S (*n* = 3–5) is presented. Trends in thermal and optoelectronic properties are studied, in dependence on the length of the conjugated backbone. Optical measurements reveal red-shifted absorption spectra and electrochemical investigations show lowering of the lowest unoccupied molecular orbital (LUMO) energy levels for DCV*n*S compared to the corresponding thiophene analogs DCV*n*T. As a consequence, a lowering of the bandgap is observed. Single crystal X-ray structure analysis of tetramer DCV4S provides important insight into the packing features and intermolecular interactions of the molecules, further corroborating the importance of the DCV acceptor groups for the molecular ordering. DCV4S and DCV5S are used as donor materials in planar heterojunction (PHJ) and bulk-heterojunction (BHJ) organic solar cells. The devices show very high fill factors (FF), a high open circuit voltage, and power conversion efficiencies (PCE) of up to 3.4% in PHJ solar cells and slightly reduced PCEs of up to 2.6% in BHJ solar cells. In PHJ devices, the PCE for DCV4S almost doubles compared to the PCE reported for the oligothiophene analog DCV4T, while DCV5S shows an about 30% higher PCE than DCV5T.

- Trimethylaluminum–Triflimide Complexes for the Catalysis of Highly Hindered Diels–Alder Reactions
  Jung, M. E.; Guzaev, M. *Org. Lett.* **2012**, *14*, 5169–5171.
  Abstract:

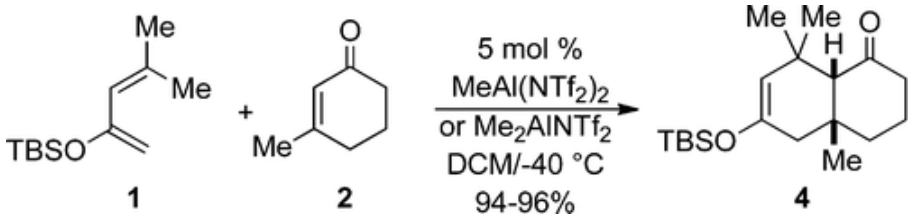

Two catalysts, Me_2AlNTf_2 and $MeAl(NTf_2)_2$, derived from the mixing of trimethylaluminum with triflimide, proved to be highly effective catalysts in hindered Diels–Alder reactions, generating the desired Diels–Alder cycloadducts from both hindered 2-silyloxydienes and hindered dienophiles. Thus reaction of 1 with 2 afforded the hindered cycloadduct 4 in excellent yield in 0.5–1.5 h at −40 °C.

- A Neutral Naphthalene Diimide [2]Rotaxane
  Jacquot de Rouville, H. P.; Iehl, J.; Bruns, C. J.; McGrier, P. L.; Frasconi, M.; Sarjeant, A. A.; Stoddart, J. F. *Org. Lett.* **2012**, *14*, 5188–5191.
  Abstract:

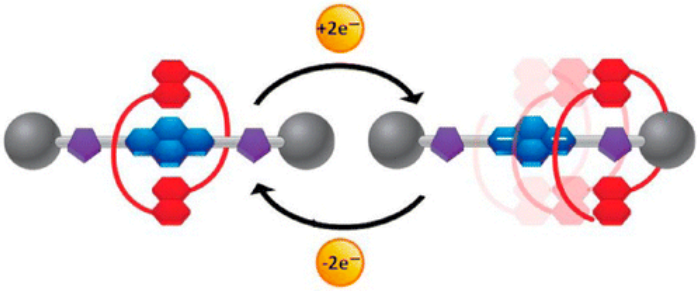

A neutral donor–acceptor [2]rotaxane, which has been synthesized using click chemistry, has had its solid-state structure and superstructure elucidated by X-ray crystallography. Both dynamic ^{1}H NMR spectroscopy and electrochemical investigations have been employed in an attempt to shed light on both geometrical reorganization and redox-switching processes that are occurring or can be induced within the [2]rotaxane.

- Plasmonic Mode Engineering with Templated Self-Assembled Nanoclusters
  Fan, J. A.; Bao, K.; Sun, L.; Bao, J.; Manoharan, V. N.; Nordlander, P.; Capasso, F. *Nano Letters* **2012**, *12*, 5318-5324.
  Abstract:

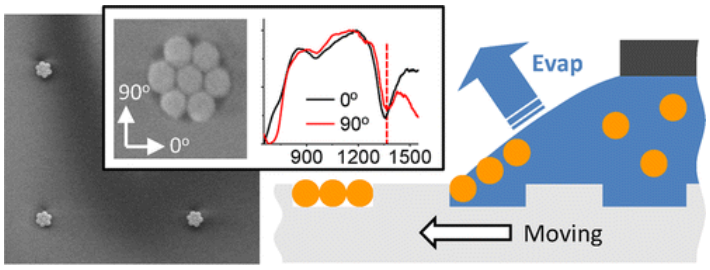

Plasmonic nanoparticle assemblies are a materials platform in which optical modes, resonant frequencies, and near-field intensities can be specified by the number and position of nanoparticles in a cluster. A current challenge is to achieve clusters with higher yields and new types of shapes. In this Letter, we show that a broad range of plasmonic nanoshell nanoclusters can be assembled onto a lithographically defined elastomeric substrate with relatively high yields using templated assembly. We assemble and measure the optical properties of three cluster types: Fano-resonant heptamers,

linear chains, and rings of nanoparticles. The yield of heptamer clusters is measured to be over 30%. The assembly of plasmonic nanoclusters on an elastomer paves the way for new classes of plasmonic nanocircuits and colloidal metamaterials that can be transfer-printed onto various substrate media.

- Capping Ligands as Selectivity Switchers in Hydrogenation Reactions
  Kwon, S. G.; Krylova, G.; Sumer, A.; Schwartz, M. M.; Bunel, E. E.; Marshall, C; L.; Chattopadhyay, S.; Lee, B.; Jellinek, J.; Shevchenko, E. V. *Nano Letters* **2012**, *12*, 5382-5388.
  Abstract:

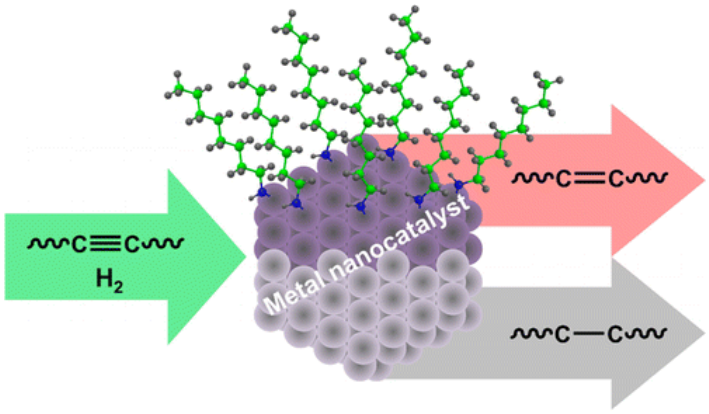

We systematically investigated the role of surface modification of nanoparticles catalyst in alkyne hydrogenation reactions and proposed the general explanation of effect of surface ligands on the selectivity and activity of Pt and Co/Pt nanoparticles (NPs) using experimental and computational approaches. We show that the proper balance between adsorption energetics of alkenes at the surface of NPs as compared to that of capping ligands defines the selectivity of the nanocatalyst for alkene in alkyne hydrogenation reaction. We report that addition of primary alkylamines to Pt and $CoPt_3$ NPs can drastically increase selectivity for alkene from 0 to more than 90% with ~99.9% conversion. Increasing the primary alkylamine coverage on the NP surface leads to the decrease in the binding energy of octenes and eventual competition between octene and primary alkylamines for adsorption sites. At sufficiently high coverage of catalysts with primary alkylamine, the alkylamines win, which prevents further hydrogenation of alkenes into alkanes. Primary amines with different lengths of carbon chains have similar adsorption energies at the surface of catalysts and, consequently, the same effect on selectivity. When the adsorption energy of capping ligands at the catalytic surface is lower than adsorption energy of alkenes, the ligands do not affect the selectivity of hydrogenation of alkyne to alkene. On the other hand, capping ligands with adsorption energies at the catalytic surface higher than that of alkyne reduce its activity resulting in low conversion of alkynes.

- Enhanced Activity of ATRP Fe Catalysts with Phosphines Containing Electron Donating Groups
  Wang, Y.; Kwak, Y.; Matyjaszewski, K. *Macromolecules* **2012**, *45*, 5911–5915.
  Abstract:

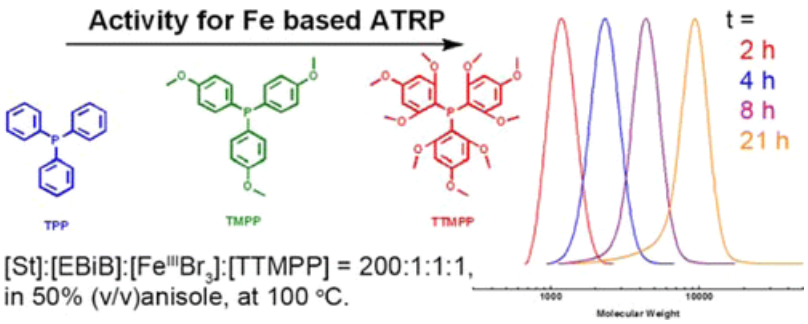

Fe-based atom transfer radical polymerization (ATRP) of styrene (St) with various triarylphosphines containing electron donating methoxy groups was investigated. $Fe^{III}Br_3$ in the presence of tris(2,4,6-trimethoxyphenyl)phosphine (TTMPP) provided faster ATRP of St than in the presence of tris(4-methoxyphenyl)phosphine (TMPP) and much faster than with triphenylphosphine (TPP) under identical conditions. ATRP of St was carried out with initial ratio of reagents: [St]:[EBiB]:[$Fe^{III}Br_3$]:[TTMPP] = 200:1:1:2, in 50% (v/v) anisole at 100 °C (EBiB is ethyl 2-bromoisobutyrate). After 21 h, conversion reached 92%, yielding polystyrene with molecular weight M_n = 24 100 and M_w/M_n = 1.25. With TMPP and TPP under the same conditions, the conversion of monomer was only 19% and 9%, respectively. With 1 equiv of TTMPP vs $Fe^{III}Br_3$, control was better, M_w/M_n ~1.1, but polymerization was slower. The phosphines could directly reduce Fe^{III} to Fe^{II} but could also act as ligands complexing transition metal and forming efficient ATRP catalysts.

- Low Bandgap Polymers Based on Silafluorene Containing Multifused Heptacylic Arenes for Photovoltaic Applications
  Yuan, M.; Yang, P.; Durban, M. M.; Luscombe, C. K. *Macromolecules* **2012**, *45*, 5934–5940.
  Abstract:

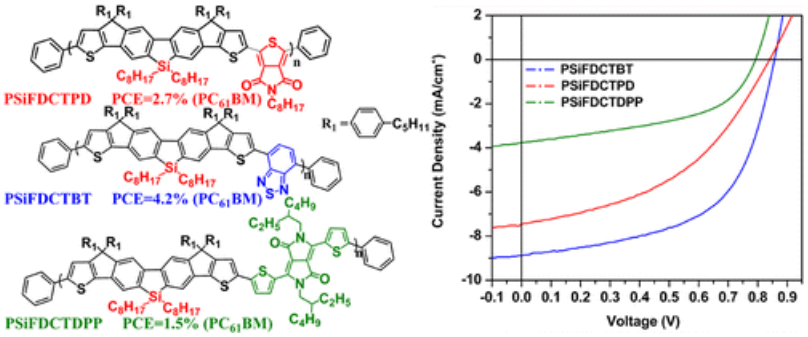

A series of donor–acceptor copolymers based on a new silafluorene containing multifused heptacylic arenes have been designed and synthesized in order to further modulate and optimize their electronic and optical properties. Polymer solar cells based on a blend of these polymers and $PC_{61}BM$ exhibited high open circuit voltages of up to 0.86 V. Through simple and straightforward engineering of molecular structures, the devices based on the PSiFDCTBT:$PC_{61}BM$ (1:3.5 in wt %) blend provided, on average, a V_{oc} of 0.86 V, a J_{sc} of 8.8 mA/cm^2, a FF of 56%, delivering a PCE of 4.2%.

- Quantitative Analysis and Characterization of Self-Assembled DNA on a Silver Surface
  Kumar, K. S.; Naaman, R. *Langmuir* **2012**, *28*, 14514-14517.
  Abstract:

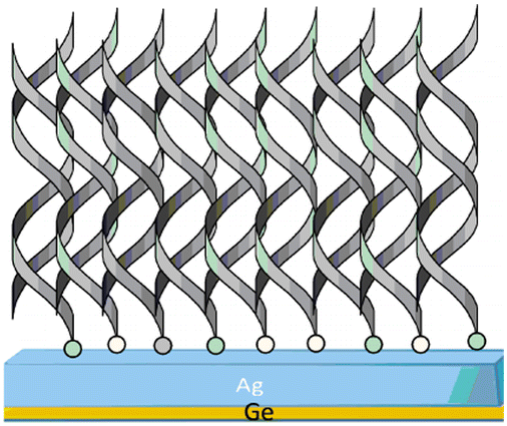

Self-assembled monolayers of DNA on a silver surface were prepared and characterized by polarization modulation infrared reflection absorption spectroscopy (PM-IRRAS), fluorescence imaging, and ^{32}P radioactive labeling. The buffer concentration of the DNA solution and the surface roughness of the silver substrate were found to affect the surface coverage of DNA and its hybridization. At low buffer concentrations, surface coverage and hybridization were greatly reduced. Ethidium bromide intercalated into the adsorbed dsDNA clearly indicates the presence of dsDNA.

- Formation of Regularly Spaced Wetting Ridges at 1 µm Intervals on the Surface of a Liquid-Crystalline Polymer
  Okuda, S.-H.; Yoshihara, S.-S.; Kang, S.; Tokita, M.; Watanabe, J. *Langmuir* **2012**, *28*, 14518-14521.
  Abstract:

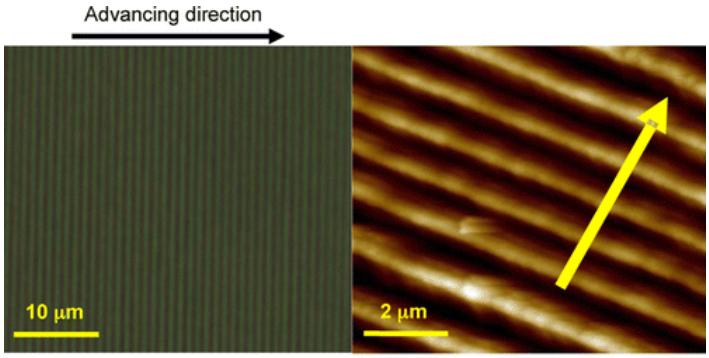

A liquid-crystalline (LC) polymer melt coating a glass support shows a remarkable wetting ridge pattern resulting from a “stick-and-break” phenomenon when submerged into water at a velocity of 20 cm/s. A series of parallel, regularly spaced wetting ridges of 0.2 µm height are formed perpendicular to the advancing direction of the plate at 1 µm intervals, and the pattern continues over a wide area (1 × 2 cm^2). The ridges function as a narrow line diffraction grating, similar to a prism that separates white light into the spectrum of colors. This process provides new insight into the controlled nanofabrication of polymers that is low-cost and high-throughput.

- Engineering polyoxometalates with emergent properties
  Miras, H. N.; Yan, J.; Long, D.-L.; Cronin, L. *Chem. Soc. Rev.* **2012**, *41*, 7403-7430.
  Abstract:

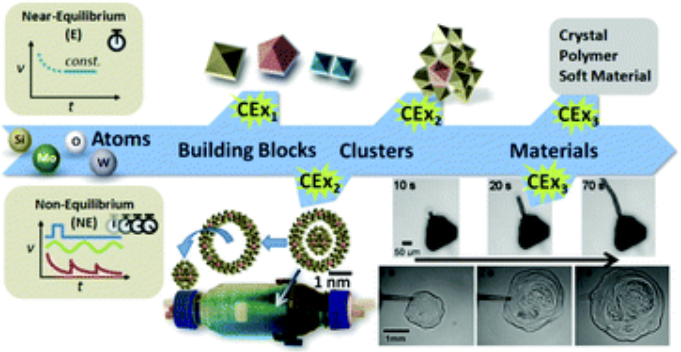

Polyoxometalates are clusters of metal-oxide units, comprising a large diversity of nanoscale structures, and have many common building blocks; in fact polyoxometalate clusters are perhaps the largest non-biologically derived molecules structurally characterised. Not only can polyoxometalates have gigantic nanoscale molecular structures, but they also a have a vast array of physical properties, many of which can be specifically 'engineered-in'. Here we describe how building block libraries of polyoxometalates can be used to construct systems with important catalytic, electronic, and structural properties. We also show that it is possible to construct complex chemical systems based upon polyoxometalates, manipulating the templating/self templating rules to exhibit emergent processes from the molecular to the macroscopic scale.

- Functionalization and post-functionalization: a step towards polyoxometalate-based materials
  Proust, A.; Matt, B.; Villanneau, R.; Guillemot, G.; Gouzerh, P.; Izzet, G. *Chem. Soc. Rev.* **2012**, *41*, 7605-7622**.**
  Abstract:

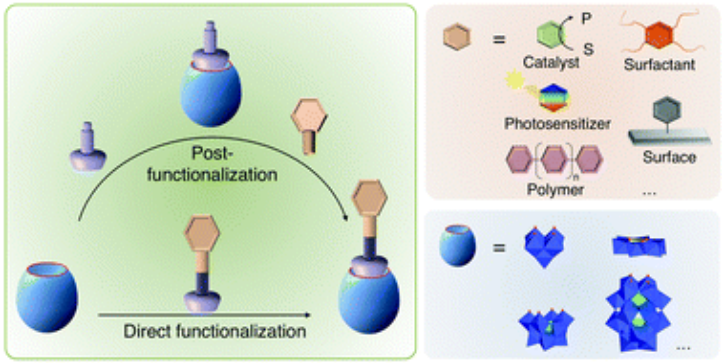

Polyoxometalates (POMs) have remarkable properties and a great deal of potential to meet contemporary societal demands regarding health, environment, energy and information technologies. However, implementation of POMs in various functional architectures, devices or materials requires a processing step. Most developments have considered the exchange of POM counterions in an electrostatically driven approach: immobilization of POMs on electrodes and other surfaces including oxides, embedding in polymers, incorporation into Layer-by-Layer assemblies or Langmuir–Blodgett films and hierarchical self-assembly of surfactant-encapsulated POMs have thus been thoroughly investigated. Meanwhile, the field of organic–inorganic POM hybrids has expanded and offers the opportunity to explore the covalent approach for the organization or immobilization of POMs. In this critical review, we focus on the use of POM hybrids in selected fields of applications such as catalysis, energy conversion and molecular nanosciences and we endeavor to discuss the impact of the covalent approach compared to the electrostatic one. The synthesis of organic–

inorganic POM hybrids starting from bare POMs, that is the direct functionalization of POMs, is well documented and reliable and efficient synthetic procedures are available. However, as the complexity of the targeted functional system increases a multi-step strategy relying on the post-functionalization of preformed hybrid POM platforms could prove more appealing. In the second part of this review, we thus survey the synthetic methodologies of post-functionalization of POMs and critically discuss the opportunities it offers compared to direct functionalization.

- Synthesis and pH-responsive micellization of brush copolymers poly(methyl methacrylate-co-2-(2-bromoisobutyryloxy)ethyl methacrylate-graft-acrylic acid): role of composition profile
  Li, J.-J.; Zhou, Y.-N.; Luo, Z.-H. *Soft Matter* **2012**, *8*, 11051-11061.
  Abstract:

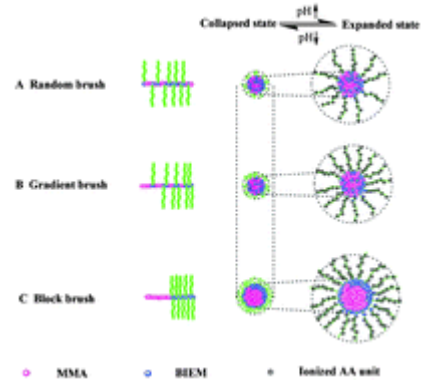

A series of brush copolymers (*i.e.* poly(methyl methacrylate (MMA)-*co*-2-(2-bromoisobutyryloxy)ethyl methacrylate (BIEM)-*graft*-acrylic acid (AA))) having three backbone composition profiles, *i.e.* random, gradient and block, were synthesized *via* the combination of atom transfer radical polymerization (ATRP)/model-based semibatch ATRcoP and the "grafting from" method. These samples allowed us to systematically investigate the effects of the composition profile (including the grafting density corresponding to the composition profile) on the micelle formation and pH responsivity of the brush copolymers in solution. FTIR, ^{1}H NMR and GPC were used to provide evidence for the formation of the well-defined brush copolymers. TEM, light transmittance and DLS were used to investigate the self-assembly and pH responsivity of the resulting copolymers. It was found that the micelles formed by these copolymers underwent a different conformational transition caused by the change from acidic to basic in the solution. These transitions were mainly influenced by pH and composition profile since the composition profile also had a strong effect on the acid-dissociation degree of the brush copolymer.

- Entropy driven polymorphism in liquids and mesophases consisting of three block amphiphilic molecules
  Peroukidis, S. D. *Soft Matter* **2012**, *8*, 11062-11071.
  Abstract:

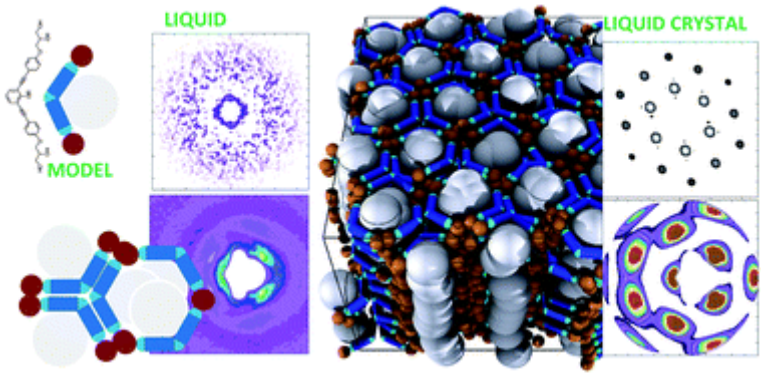

The phase behavior and the structure of athermal systems consisting of amphiphilic three-block molecules are studied using Monte Carlo molecular simulations. A coarse grain molecular prototype is introduced that mimics the very basic features of real bola and facial T- and V-shaped amphiphilic liquid crystals. Entropy driven phase polymorphism of liquids and liquid crystals is obtained by varying the size and/or the shape of the lateral block of the molecules. Such polymorphism includes non-conventional smectics, columnars and hierarchical lamellar phases. The results indicate that the isotropic liquids possess different local order; the geometry of the most probable local molecular order (molecular domain) in the liquid offers a natural explanation for the type of the observed mesophase(s). These findings provide a coherent bottom up interpretation of the diversity of the phases exhibited by amphiphilic liquid crystals.

- Macroporous nanowire nanoelectronic scaffolds for synthetic tissues
  Tian, B.; Liu, J.; Dvir, T.; Jin, L.; Tsui, J. H.; Qing, Q.; Suo, Z.; Langer, R.; Kohane, D. S.; Lieber, C. M. *Nature Materials* **2012**, *11*, 986–994.
  Abstract:

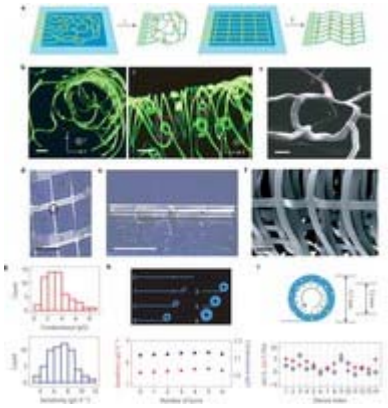

The development of three-dimensional (3D) synthetic biomaterials as structural and bioactive scaffolds is central to fields ranging from cellular biophysics to regenerative medicine. As of yet, these scaffolds cannot electrically probe the physicochemical and biological microenvironments throughout their 3D and macroporous interior, although this capability could have a marked impact in both electronics and biomaterials. Here, we address this challenge using macroporous, flexible and free-standing nanowire nanoelectronic scaffolds (nanoES), and their hybrids with synthetic or natural biomaterials. 3D macroporous nanoES mimic the structure of natural tissue scaffolds, and they were formed by self-organization of coplanar reticular networks with built-in strain and by manipulation of 2D mesh matrices. NanoES exhibited robust electronic properties and have been used alone or combined with other biomaterials as biocompatible extracellular scaffolds for 3D culture of neurons, cardiomyocytes and smooth muscle cells. Furthermore, we show the integrated sensory capability of

the nanoES by real-time monitoring of the local electrical activity within 3D nanoES/cardiomyocyte constructs, the response of 3D-nanoES-based neural and cardiac tissue models to drugs, and distinct pH changes inside and outside tubular vascular smooth muscle constructs.

- Bulk electronic structure of the dilute magnetic semiconductor Ga1−xMnxAs through hard X-ray angle-resolved photoemission
  Gray, A. X.; Minár, J.; Ueda, S.; Stone, P. R.; Yamashita, Y.; Fujii, J.; Braun, J.; Plucinski, L.; Schneider, C. M.; Panaccione, G.; Ebert, H.; Dubon, O. D.; Kobayashi, K.; Fadley, C. S. *Nature Materials* **2012**, *11*, 957–962.
  Abstract:

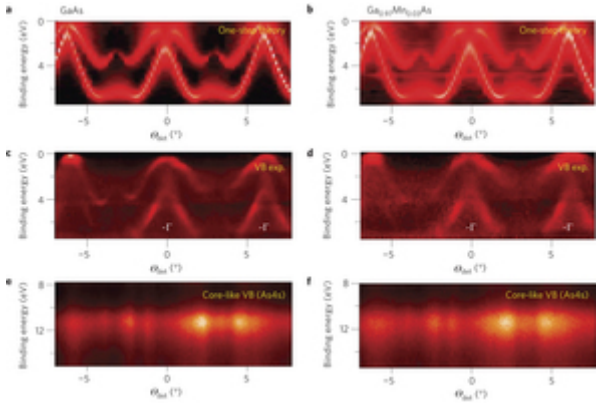

A detailed understanding of the origin of the magnetism in dilute magnetic semiconductors is crucial to their development for applications. Using hard X-ray angle-resolved photoemission (HARPES) at 3.2 keV, we investigate the bulk electronic structure of the prototypical dilute magnetic semiconductor Ga0.97Mn0.03As, and the reference undoped GaAs. The data are compared to theory based on the coherent potential approximation and fully relativistic one-step-model photoemission calculations including matrix-element effects. Distinct differences are found between angle-resolved, as well as angle-integrated, valence spectra of Ga0.97Mn0.03As and GaAs, and these are in good agreement with theory. Direct observation of Mn-induced states between the GaAs valence-band maximum and the Fermi level, centred about 400 meV below this level, as well as changes throughout the full valence-level energy range, indicates that ferromagnetism in Ga1−xMnxAs must be considered to arise from both p–d exchange and double exchange, thus providing a more unifying picture of this controversial material.